Influence of the paste volume on the contact formation in fine line metallization

Dominik Rudolph[1], Adrian Adrian[1], Jan Lossen[1], Pablo Ferrada[2], Carlos Portillo[2], Valeria del Campo[3], Jonathan Correa[3], Rodrigo Sierpe[4] and Marcelo Javier Kogan[4]

[1]ISC Konstanz, Rudolf-Diesel Str. 15, 78467 Konstanz, Germany

[2]Centro de Desarrollo Energético Antofagasta, Universidad de Antofagasta, Antofagasta #0601, Chile

[3]Departamento de Física, Universidad Técnica Federico Santa Maria, Av. España 1680, Valparaíso, Chile

[4]Departamento de Química Farmacológica y Toxicología , Universidad de Chile, Av. Santos Dumont 964 Independencia, Santiago de Chile

***Abstract* — Metallization of industrial silicon solar cells is evolving towards fine line printing with a line width of 30 µm and lower. Besides the challenge to keep up a high aspect ratio this might also result in higher contact resistivities. This work investigates the influence of the paste volume on the contact formation for fine line metallization. It is shown that the paste volume has an influence on the contact resistivity. But it depends on the used paste if this influence is detrimental or advantageous for the contact formation on reduction of the paste volume.**

I. Introduction

Due to its importance in improving silicon solar cells the contact formation of thick film Ag contacts has been investigated for many years. It was shown by several research groups that the main contact is achieved by silver crystallites grown into silicon [1-4]. The formation of these crystallites is strongly influenced by the amount of oxygen in the firing ambience, the solar cell surface topography, the fraction of inactive dopants in the surface, the firing profile and the cooling rate after firing [5-8]. Besides the contact achieved by silver crystallites in direct contact with bulk Ag, it is proposed, that the current can also flow by multi tunneling between the silver colloides suspended in the interfacial glass. Mikeska et al. have proclaimed that the current flows via Ag crystallites, multi tunneling through colloidal Ag precipitates and an ultra-thin interfacial glass layer and hence all three mechanism contribute to a good contact [9]. Before Ag crystallites can be formed and Ag could precipitate inside the glass, the silicon nitride passivation layer has to be etched at least partially. This process is influenced by the kind of glass frit, the fraction of glass and the size of the silver particles [3], [10], [11].

Photovoltaic industry is moving towards finer metal lines on the front side of conventional solar cells and for the rear side of bifacial solar cells. Less shading and lower contact recombination are opportunities of finer metal lines but the main opportunity is the cost reduction due to reduced silver paste consumption. The main challenge in going to finer lines is keeping up a high aspect ratio while reducing the finger width. However even if the aspect ratio is high, the paste volume in comparison to a broader screen printed finger is lower. The main scope of this work is to investigate the influence of paste volume on the contact formation for different cell concepts. In previous double printing experiments one of the conclusions was that the contact resistivity is influenced by the paste amount [12]. The question is if there is a critical paste amount limit where the contact formation is hindered? What influence has the cell surface topography, the surface doping and the paste formulation?

II. Experimental

To achieve data for different surface topographies two types of cells were processed for the experiments: monocrystalline p-type PERC cells with alkaline texture and n-type bifacial PERT cells with flat rear side. The PERC cells are made by first alkaline saw damage etch with an adjacent cleaning step. Then the rear side is passivated by plasma-enhanced chemical vapor deposition (PECVD).

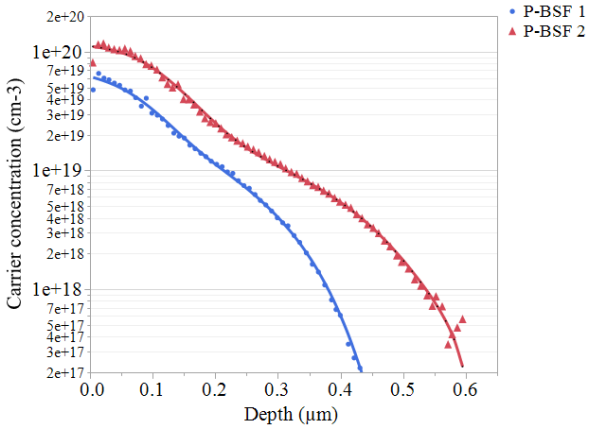

Fig. 1. ECV measurement of the BSF on the rear side of the n-PERT cells of group 1,2, 4 and 5.

The front surface is subsequently textured in an alkaline solution. Phosphorous diffusion is done in in a quartz tube

TABLE I
GROUP PLAN

Group	Cell							
	type	size	Front side			Rear side		
			topography	doping	metallization	topography	doping	metallization
1	n-type cz PERT	156.75	Alkaline textured	Boron	AgAl p+ paste	flat	P-BSF 1	Ag paste A
2	n-type cz PERT	156.75	Alkaline textured	Boron	AgAl p+ paste	flat	P-BSF 2	Ag paste A
3	p-type cz PERC	156.75	Alkaline textured	P-Emitter 95Ω/sq	Ag paste A		-	Local Al-
4	n-type cz PERT	156.75	Alkaline textured	Boron	AgAl p+ paste	flat	P-BSF 1	Ag paste B
5	n-type cz PERT	156.75	Alkaline textured	Boron	AgAl p+ paste	flat	P-BSF 2	Ag paste B

furnace containing $POCl_3$.After phosphorous glass etching the front side is passivated by PECVD SiN_x. The rear side is locally opened by a green Nd:YAG laser with a pulse duration in ns range. The rear side is metallized with full area Al and the front side fingers are printed with a commercial Ag paste A using a screen with 100 fingers and 20 µm opening. To achieve different paste volumes while not increasing the contacting area this print is repeated up to four times with subsequent drying. Afterwards the cells are co-fired in a belt furnace.

The PERT cells are made of 6-inch n-type monocrystalline Si <100> wafers (244.31 cm^2) with base resistivity of 5 to 5.9 Ωcm by using only standard industrial processes. After alkaline saw damage etching all wafers are cleaned. Two different diffusion profiles are used to create the n^+ back surface field (BSF) in a quartz tube furnace containing $POCl_3$. These profiles, measured by ECV, are plotted in Figure 1. After the diffusion step a silicon nitride layer is deposited by PECVD on the rear side. All wafers are textured using a wet chemical alkaline process and a subsequent cleaning step. The emitter is diffused in a quartz tube furnace containing BBr_3. A stack of thermal SiO_2/PECVD-SiN_x on the front side serves as passivation and antireflective coating. For metallization the cells are sorted into different groups. The front side metallization, by AgAl p^+ paste is kept the same for all n-type PERT groups using 100 fingers with 35 µm opening and five bus bars. The rear side of group 1 and 2 is printed with commercial Ag paste A and the rear side of group 4 and 5 is printed with commercial Ag paste B using a screen with 100 fingers and 20 µm line opening. This print is repeated up to three times with subsequent drying. The groups are listed in Table I. After co-firing in a belt furnace the bus bar interconnection on the rear side is done via screen printing of a low temperature Ag paste.

From all cells the IV curve was measured in a h.a.l.m flasher. Afterwards the topography and the line shape was determined using a laser scanning microscope (LSM). Some cells were chosen and cut into stripes with 1 cm width and then the contact resistivity was determined using the transmission line method

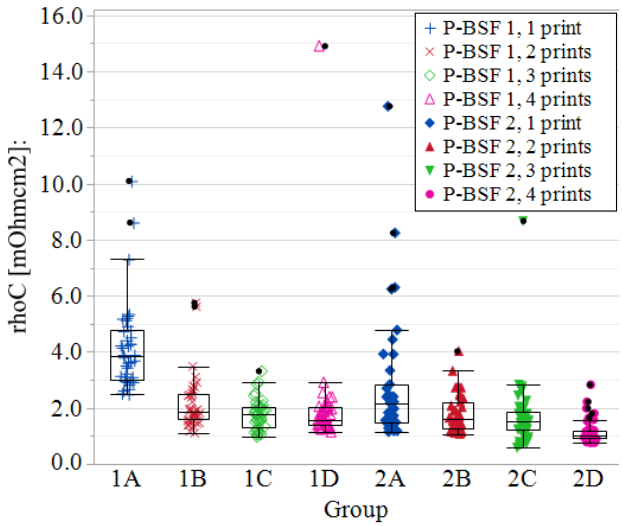

Fig. 2. TLM measurement results of group 1 and 2. Ag paste A printed up to four times on the flat rear side with p-BSF 1 and 2.

TABLE II
IV RESULTS

Group	Mean J_{SC} ($mAcm^2$)	Mean V_{OC} (V)	Mean FF (%)	Mean η (%)
1A	39.09	0.657	78.06	20.05
1B	39.10	0.657	78.72	20.21
1C	39.18	0.658	78.73	20.28
1D	39.16	0.657	79.15	20.36
2A	38.97	0.650	78.34	19.84
2B	38.95	0.649	79.40	20.07
2C	38.93	0.649	79.31	20.04
2D	38.99	0.650	79.37	20.12
3A	38.54	0.663	72.15	18.44
3B	38.88	0.660	75.17	19.28
3C	38.67	0.662	78.67	20.13
3D	38.97	0.661	78.72	20.27
3E	38.90	0.662	78.14	20.13
4A	39.01	0.655	67.25	17.17
4B	39.00	0.653	75.88	19.33
4C	39.14	0.656	76.67	19.70
5A	38.92	0.649	74.95	18.93
5B	38.91	0.648	77.23	19.48
5C	38.93	0.648	77.19	19.48

(TLM). To investigate the contact area by scanning electron microscopy (SEM) these stripes were etched back by first using HNO_3 to remove the silver bulk, then using HF to remove the glass layer and at the end using again HNO_3 to remove the remaining silver crystallites and precipitates.

III. Results

The IV results are summarized in Table II. The number of print on print steps is marked with the letters A to E, meaning A is single print, B is double print and further on. It is obvious that for all groups the FF is increasing with higher number of prints. Part of the FF improvement is due to the increased line conductivity, which is summarized in the last column of Table III. But this is not explaining the full change in FF. Hence the contact resistivity is also influenced by the amount of paste printed on the cell. The V_{OC} and J_{SC} are not decreasing with increasing number of prints, which proves the fact that the contacting area is not significantly increased, otherwise the recombination and the shading would be expected to increase. LSM measurement results of the metal fingers are summarized in Table III. The line width changes slightly but not significantly with increased number of prints but the height and hence the cross section are increasing proportionally. Therefore the line resistivity is decreasing accordingly.

TABLE III
LINE GEOMETRY AND LINE RESISTIVITY

group	Mean line height (µm)	Mean line width (µm)	Line cross section (µm²)	Mean line resistivity (Ωcm)
1A & 2A	7.8	51	322	0.87
1B & 2B	17.0	51	568	0.44
1C & 2C	21.7	52	733	0.34
1D & 2D	27.6	53	904	0.29
3A	9.4	46	420	0.83
3B	12.9	41	512	0.68
3C	15.7	40	581	0.49
3D	18.0	43	727	0.37
3E	21.8	42	755	0.24
4A & 5A	12.3	41	388	0.88
4B & 5B	22.3	45	663	0.51
4C & 5C	28.7	49	898	0.38

Figure 2 shows the measured contact resistivity ρ_C for all n-type PERT cells printed with paste A. The groups differ in doping profile and amount of print on print steps. For both group 1 and 2, the contact resistivity steadily decreases by increasing paste amount and hence paste volume. The doping profile of the BSF has only a minor influence.

Figure 3 shows the contact resistivity of Ag paste A on the textured front side of the p-type PERC cells. Here the effect of the paste amount is not as clear as for the group 1 and group 2. But a trend is visible that the variation is decreasing for increasing paste amount until up to four print on print steps. After five print on print steps the contact resistivity and its

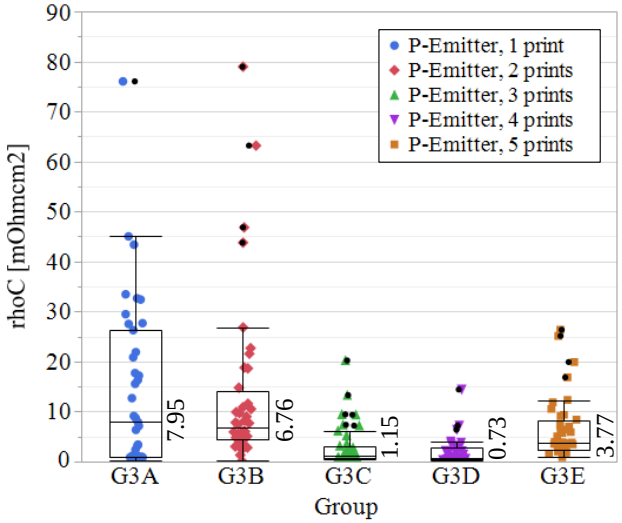

Fig. 3. TLM measurement results of Ag paste A printed up to five times on the textured front side of the PERC cells.

variation increases again.

The contact resistivity of Ag paste B on flat P-BSF is shown in Figure 4. For group 4 and 5, both paste B, the effect on the contact resistivity by increasing paste amount is opposite than for the groups 1, 2 and 3. Overall the contact resistivity with paste B is significantly higher than with paste A which is the reason for the lower FF values of group 4 and 5.

In order to understand this phenomenon, SEM measurements of cross sections show that by increasing the paste volume more

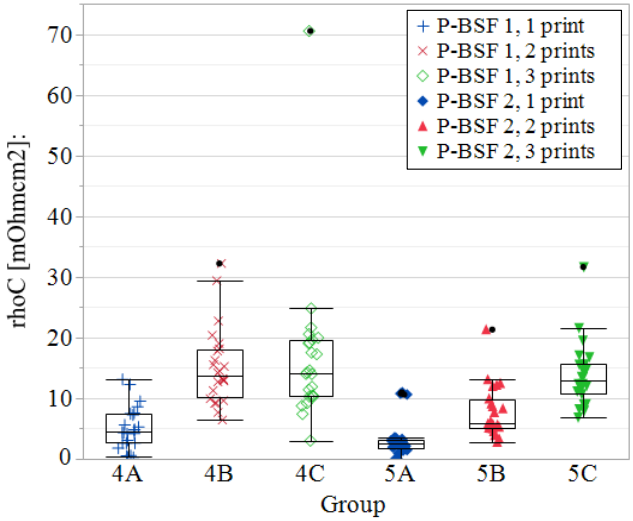

Fig. 4. Contact resistivity of Ag paste B printed on the flat rear side of the n-type PERT cells, measured by TLM method.

and more glass is agglomerated together and builds thick glass layers like it is shown in Figure 5. These glass layers contain a lot of metal precipitates, but due to their thickness current flow between Si surface and Ag bulk is most presumably hindered.

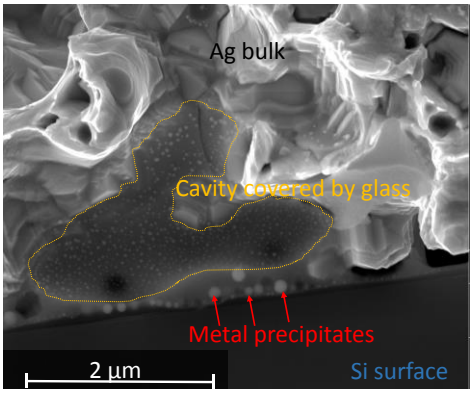

Fig. 5. SEM cross section image of a sample, which was printed three times with paste B. A big cavity covered by glass is found directly between Si surface and Ag bulk.

Further, we compared the sample surfaces after HNO_3 and HF etching as well after subsequent HNO_3 etching of group 1A and 4A. Figure 6 shows the surfaces of group 1A on the left side and of group 4A on the right side. After HNO_3 and HF etching, shown in Figure 6 a) and b), the silver crystallites are visible, which are normally covered by the glass layer. Here we see that paste A results in a higher crystallite density than paste B, which obviously explains the slightly lower contact resistivity of paste A for the single print case. Figure 6 c) to f) show the surface after all etching steps. According to the work of Mette the fraction of etched SiNx-layer was determined on three images for each paste [13]. For paste A the mean value for the etched SiNx-layer is 49%, while for paste B it is 68%. Hence paste B contains either a higher amount of glass frit or a glass frit with lower T_g, which is more aggressive. This explains also the lower V_{OC} of the samples printed with paste B in comparison to the samples printed with paste A. The comparison of Figure 6 e) with f) shows beside the higher silver crystallite density for paste A also deeper etching pits. An effect on the recombination current J_{02} of these pits is not seen. J_{02} for group 1A is around 37.51 nA/cm^2 and increases slightly with increasing paste amount with its maximum at group 1C of 39.71 nA/cm^2. For group 4A J_{02} is 38.43 nA/cm^2, for group 4B it is 41.68 nA/cm^2 and for group 4C it is 38.77 nA/cm^2. Which proves that the pits, which we see in Figure 6 e) and f), do not penetrate the n-p junction and do not reach into the space charge region (SCR).

IV. Discussion & Conclusion

The surface topography and the paste volume have an influence on the contact resistivity for both paste A and paste B, while the two tested diffusion profiles of the BSF have only a minor influence. For paste A the contact resistivity is decreasing with increasing paste volume until a certain amount is reached. If the paste volume is increased further we can see in case of group 3 that ρ_C is increasing again. The glass frit contained in the paste is melted during firing and wets the cell surface but if the paste volume is low it could be that glass frit amount is not sufficient enough to enable good contact formation. Hence by increasing the paste volume this shortage can be overcome.

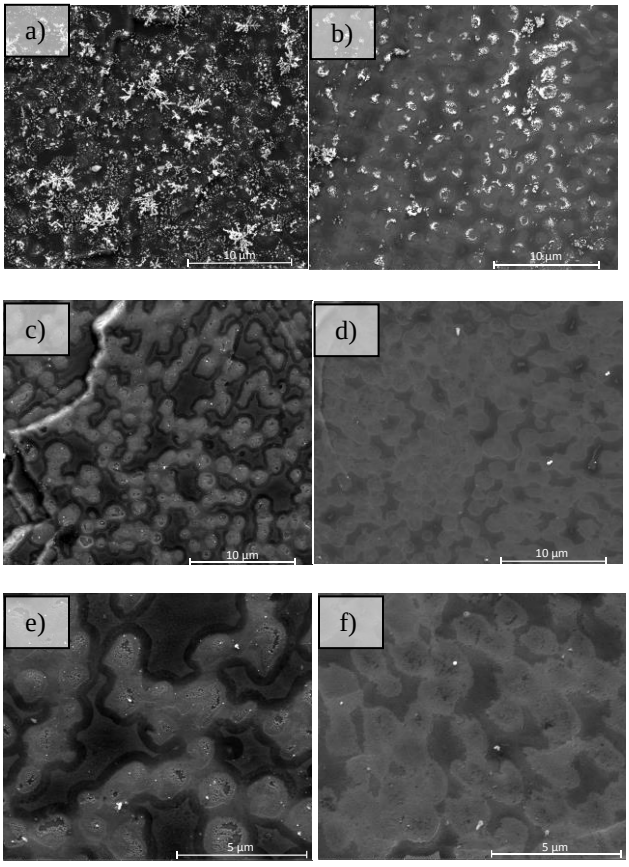

Fig. 6. SEM images for group 1A on the left side and group 4A on the right side. The upper images a) and b) show the surface after HNO_3 and HF etching while the lower images c) to f) show the surface after HNO_3, HF and HNO_3 etching.

For paste B the behavior of ρ_C in dependency of the finger paste volume is opposite. An increase in ρ_C with increasing finger paste volume is visible for both BSF types. The formulation of paste B is different than that of paste A and our assumption is that the glass frit contained in paste B is more aggressive or its share is higher than in paste A so that even at low paste amount it is sufficient to open the passivation layer and enhance the contact formation. With increasing paste amount the interfacial glass thickness increases, which acts as an insulation layer between Si surface and Ag bulk, and hence the contact resistivity is increasing.

Pastes for fine line printing have to be divided by their purpose in two categories:

- Case 1: fine line print with low paste volume for multi BB approach, double print and for seed layer
- Case 2: fine line print with high aspect ratio for single print and up to six BB

For case 1 a higher amount of glass frit is needed than for standard pastes to obtain sufficient SiN_x etching. It behaves different for case 2, where a lower amount of glass frit with high transport behavior is sufficient. Eberstein et al. has reported that the amount of paste glass taking part in the interface reactions is strongly determined by its transport behavior in the pastes microstructure during firing [11]. If the paste volume is too high, the paste contains a glass with low transport behavior or the silver particles are sintering too fast during firing the contact formation will be obviously hindered. Further Khadilkar et al. has reported that with increased glass fluidity the Ag mobility and the Ag solubility is increased, which results in increased Ag-Si coverage of the surface [7]. For instance, a higher PbO content in the glass has a negative influence on the glass viscosity [3]. Hence, glasses with higher PbO content could be one solution to support the wetting of cell surface for case 2.

We conclude that lowest contact resistance is achieved for a specific paste volume, which is different for each paste. Hence, when the finger volume is reduced, especially for approaches using double printing or new printing techniques with very low laydown, the glass content and formulation in the paste needs to be adjusted.

REFERENCES

[1] G. Schubert, F. Huster and P. Fath, "Current transport mechanism in printed Ag thick film contacts to an n type emitter of a crystalline silicon solar cell," in *Proceedings 19th EUPVSEC*, Paris, France, pp. 813-816, 2004.

[2] G. Schubert, F. Huster and P. Fath, "Physical understanding of printed thick-film front," *Solar Energy Materials & Solar Cells 90,* pp. 3399-3406, 2006.

[3] K.-K. Hong, S.-B. Cho, J.-Y. Huh, H. J. Park and J.-W. Jeong, "Role of PbO-based glass frit in Ag thick-film contact formation for crystalline Si solar cells," *Met. Mater. Int., Vol. 15, No. 2,* pp. 307-312; DOI: 10.1007/s12540-009-0307-3, 2009.

[4] M. Hoerteis, T. Gutberlet, A. Reller und S. W. Glunz, „High-Temperature Contact Formation on n-Type Silicon: Basic Reactions and Contact Model for Seed-Layer Contacts," *Advanced Functional Materials 20,* pp. 476-484; DOI: 10.1002/adfm.200901305, 2010.

[5] S.-B. Cho, K.-K. Hong, J.-Y. Huh, H. J. Park und J.-W. Jeong, „Role of the ambient oxygen on the silver thick-film contact formation for crystalline silicon solar cells," *Current Applied Physics 10,* pp. 222-225, 2010.

[6] E. Cabrera, S. Olibet, D. Rudolph, J. Glatz-Reichenbach, E. Wefringhaus, R. Kopecek, D. Reinke and G. Schubert, "Influence of Surface Topography on the Glass Coverage in the Contact Formation of Silver Screen-Printed Si Solar Cells," *IEEE Journal of Photovoltaics Volume 3 Issue 1,* pp. 102-107, 2013.

[7] C. Khadilkar, S. Sridharan, D. Gnizak, T. Pham, S. Kim und A. Shaikh, „Effect of glass chemistry and silicon orientation on the front contact microstructure formation in a silicon solar cell," in *20th European Photovoltaic Solar Energy Conference*, Barcelona, Spain, pp. 1291-1296, 2005.

[8] P. Ferrada, C. Portillo, V. del Campo, E. Cabrera, D. Rudolph, M. Ponce Bustos, M. J. Kogan and R. Kopecek, "Metallization of a Lightly Doped Emitter With Different Industrial Silver Pastes: Performance and Microscopy Analysis," *IEEE JOURNAL OF PHOTOVOLTAICS, VOL. 7, NO. 3,,* pp. 727-734, 2017.

[9] K. R. Mikeska, A. F. Carroll, L. K. Cheng and Z. Li, "Screen-printed silver contact mechanisms," in *28th European Photovoltaic Solar Energy Conference and Exhibition*, Paris, France, pp. 39-42, 2013.

[10] M. M. Hilali, S. Srinivasan, C. Khaldilkar, A. Shaikh, A. Rohatgi und S. Kim, „Effect of Glass Frit Chemistry on the Physical and Electrical Properties of Thick-Film Ag Contacts for Silicon Solar Cells," *Journal of ELECTRONIC MATERIALS, Vol. 35, No. 11,* pp. 2041-2047, 2006.

[11] M. Eberstein, J. Schilm, K. Reinhardt and U. Partsch, "Kinetic aspects of the contact formation by glass containing silver paste," in *Proceedings of the 27th European Photovoltaic Solar Energy Conference and Exhibition*, Frankfurt, Germany, pp. 840-844, 2012.

[12] J. Lossen, D. Rudolph, L. Koduvelikulathu, R. Carvalho, M. Rossetto, O. Borsato, E. Bortoletto und M. Galiazzo, „Double printing nPERT cells with narrow contact layers," *Energy Procedia vol. 92,* pp. 939-948, 2016.

[13] A. Mette, New Concepts for Front Side Metallization of Industrial Silicon Solar Cells, Freiburg im Breisgau: URN: urn:nbn:de:bsz:25-opus-37820, 2007.